



HAL
open science

Modeling and pre-installation stability assessment of a real grid-connected MV DC microgrid with 100% power electronics based generation

Sameh Betamony, Jérôme Buire, Seddik Bacha, Thai-Phuong Do, Anthony Bier, Quoc Tuan Tran

► To cite this version:

Sameh Betamony, Jérôme Buire, Seddik Bacha, Thai-Phuong Do, Anthony Bier, et al.. Modeling and pre-installation stability assessment of a real grid-connected MV DC microgrid with 100% power electronics based generation. ISGT EUROPE 2023 - IEEE PES Innovative Smart Grid Technologies Europe, Oct 2023, Grenoble, France. pp.1-5, 10.1109/ISGTEUROPE56780.2023.10407355 . hal-04912684

HAL Id: hal-04912684

<https://hal.science/hal-04912684v1>

Submitted on 26 Jan 2025

HAL is a multi-disciplinary open access archive for the deposit and dissemination of scientific research documents, whether they are published or not. The documents may come from teaching and research institutions in France or abroad, or from public or private research centers.

L'archive ouverte pluridisciplinaire **HAL**, est destinée au dépôt et à la diffusion de documents scientifiques de niveau recherche, publiés ou non, émanant des établissements d'enseignement et de recherche français ou étrangers, des laboratoires publics ou privés.

Modeling and Pre-installation Stability Assessment Of a Real Grid-connected MV DC Microgrid With 100% Power Electronics Based Generation

Sameh Betamony^{1,2}

Jérôme Buire¹

Seddik Bacha¹

¹Univ. Grenoble Alpes, CNRS, Grenoble INP, G2Elab
F-38000 Grenoble, France
sameh.betamony@cea.fr

Thai-Phuong Do²

Anthony Bier²

Quoc Tuan Tran²

²Univ. Grenoble Alpes, CEA Liten, INES,
73375 Le Bourget du Lac,

Abstract— This paper proposes a pre-installation stability assessment for a real test case of a 100% power electronics-based DC microgrid in the lack of some equipment models. The approach includes dynamical modeling and parameter tuning of the microgrid components, system stability and behavior analysis under different scenarios using simulation tools. The findings from this analysis may help system designers and operators identify potential stability challenges and identify critical operational conditions, which might require verification when connecting attempting real connection.

Index Terms— Control, DC microgrids, Modeling, Stability

I. INTRODUCTION

Since their introduction [1], Microgrids are stepping in as a major player in the energy transition as a promising solution that offers different features such as the ability to work in both grid-connected mode and islanded mode. In addition to that, and with the rapid development of power electronics technology, grid-connected DC microgrids are gaining more and more attention [2][3], especially since most of the modern loads are DC by nature [4]. On the other hand, DC microgrids offer systems with fewer conversion steps, thus higher efficiency. Another factor increasing DC microgrids popularity is the network's control architecture simplifying compared to AC networks.

Recognizing the potential of hybrid DC-microgrids, the TIGON European project [5] [6] is one of the big projects that

aims to demonstrate the advantages of hybrid DC-based microgrids. Different real case demos are planned to be implemented and one of them will be in collaboration with the French Alternative Energies and Atomic Energy Commission (CEA). Although every piece of equipment went through different stability tests individually, system-level tests have to be done to make sure stability boundaries are respected. This paper investigates part of the efforts to evaluate microgrid stability and discusses different challenges in conducting the analysis. The test case architecture is illustrated in Figure 1. The test network consists of an AC/DC inverter (inverter number 1) which connects the DC side of the microgrid (3 kV) to the AC side (three-phase 400V grid). In the second stage, a DC/DC converter (converter number 2) steps down the voltage from 3 kV to 1.4 kV where there is a 50kWp PV farm connected through a DC/DC converter (converter number 3) and an AC 50 kW load connected through a DC/AC inverter (inverter number 4).

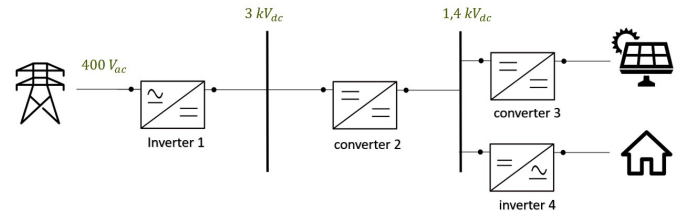


Figure 1 Network architecture

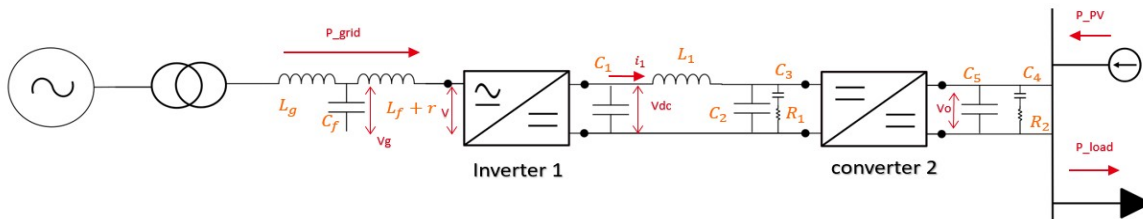


Figure 2 Microgrid model on Simulink

A pre-installation stability analysis of the test case is essential to realize a good sizing and avoid any failure or equipment's damage. Different challenges are present, First challenge is linked to the modeling. Indeed, the test case microgrids' main elements can be divided into three categories: 1) In-house designed inverters such as inverter number 2, where it's possible to obtain the detailed model for stability analysis, and also possible to modify some control parameters to achieve higher stability margins; 2) Equipment developed by external research partner, such as inverter number 1, with no detailed model is available, and it can be difficult to do changes to control parameters; 3) Commercial products such as inverters number 4 and 5 where it's not possible to get neither the detailed model and nor control modifications.

The second major challenge is linked to the lack of standardized stability requirements for DC microgrids. Due to their special characteristics, an effort was made [7] to classify stability issues in microgrids. While different standards investigate stability requirements in AC grid-connected microgrids such as IEEE 1547, to the knowledge of the writers, few of them address DC microgrids. Focusing on these two challenges, we aim here to establish a framework to assist the stability of the test case microgrid.

The rest of the paper will be organized as follows: Section 2 will present the equipment's simulation models and their validation. Section 3 will present simulation stability analysis using two test scenarios, section 4 will discuss conclusions and future works.

II. MODELS

Matlab Simulink® is used to model the microgrid as shown in Fig. 2 . Grid impedance parameters used in the model are listed in the following table 1.

Element	Value
Lg, Lf, L1	0.45 mH, 2.6 mh, 10 mh
Cf, C1, C2, C3, C4, C5	20, 1360, 25, 8, 100, 32 microF
R1, R2	10, 2.5 ohms

Table 1: Impedance parameter

Component models of the different devices will be detailed in the next sections. Modeling will focus specifically on the dynamic behavior of two main converters (Inverter 1 and Converter 2) which affect strongly the DC buses voltage stability. Other components such as PV and load are modelled by a simpler approach.

A. Inverter 1

Inverter 1 is a 300 kW solid-state transformer, which is developed in the frame of the TIGON project by the institute CIRCE. As previously mentioned, this inverter's main role is to play an interface between AC main grid and DC micro grid, maintain the MV DC grid voltage, and the active/reactive power from the AC grid. In our analysis, we focus on the objective of the DC link voltage control, for a reason the inverter will be modeled as a voltage source grid-

connected inverter with an LC filter. Figure 3 shows the adapted control loop for inverter 1, the adapted control strategy is based on [8] and uses a cascaded loop control. An outer loop (voltage controller) with a PI controller, which compares the DC link referenced voltage with the measured one and evaluates a reference d frame current. In addition, an Inner loop (Current controller) with a PI controller that controls the current in the output filter inductance. For the stability analysis, we assumed a unity power factor, hence; the Q frame current reference is fixed at zero. For synchronization, we assumed the widely used SRF PLL[9].

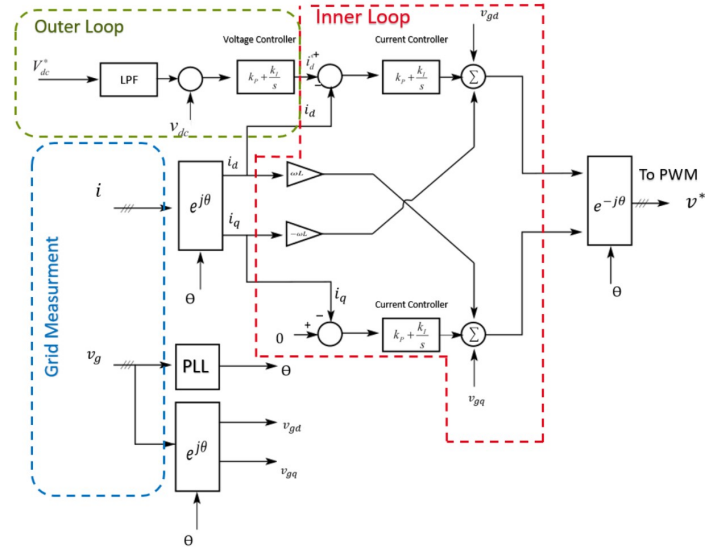


Figure 3 Adapted control loop for inverter 1

For the inner loop, the main control object is to control the current in the inductance, hence using the following differential equations represents the dynamics of the current in both d and q frames:

$$L_f \frac{di_d}{dt} = -v_d + i_d r + v_{gd} - \omega i_q L_f \quad (1)$$

$$L_f \frac{di_q}{dt} = -v_q + i_q r + v_{gq} + \omega i_d L_f \quad (2)$$

Where v_d and v_q are the d and q frame components of the grid voltage, i_d and i_q are the d and q frame components of the grid current. Based on linearization and Laplace transformation we can use the small signal model shown in figure 4 for tuning purposes :

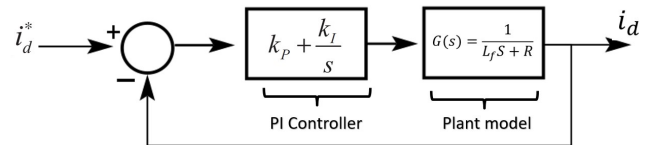


Figure 4 small-signal model for the inner control of inverter 1

For inner loop, control parameter values obtained after tuning is $K_p = 0.45$ and $K_i = 232$.

Concerning the outer loop [8], a relationship between the output current and the input voltage was derived to obtain the small signal model.

$$\frac{3}{2}(v_{gd}i_d + v_{gq}i_q) = -v_{dc}C_1 \frac{dv_{dc}}{dt} + v_{dc}i_1 \quad (3)$$

Note that the left hand part of equation 3 represents the input power from the grid side, and the right hand term represents the output power on the DC side. V_{dc} is the input dc link voltage, C_1 represents the capacitance of the dc link and finally i_1 represents the output current in the dc side. Linearizing the above equation and applying Laplace transformation, a relation between the d components of the grid current and the DC link voltage can be established and a plant model can be derived, where $R_o = V_o/I_o$ (at the operation point). A closed loop small signal model shown in figure 5 can then be used to tune the controllers.

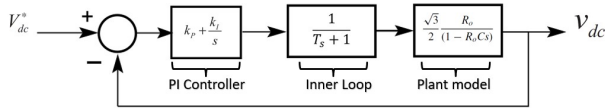


Figure 5 Small-signal model for the outer loop of inverter 1

For outer loop, control parameter values obtained after tuning $K_p = -0.8$ and $K_i = -16$.

Since there are no clear specifications on the dynamical response of the inverter, the only constraint we used is to have a much smaller bandwidth of the outer loop than the inner loop, to decouple the dynamics of the two loops avoiding stability problems[10]. Hence; outer loop was tuned to be 10 times slower than the inner loop allowing us to represent it as a first order transfer function with a time constant T_s in the small signal model for the outer loop.

Finally, the simulation model of inverter 1 was verified using a test case where we reversed the power flow at $t=1$ sec and observed the voltage on the 3 kV DC link as can be seen in figure 6.

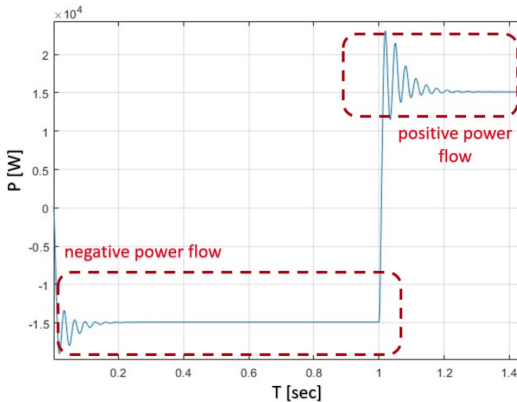


Figure 6 Power flow dynamics for inverter 1

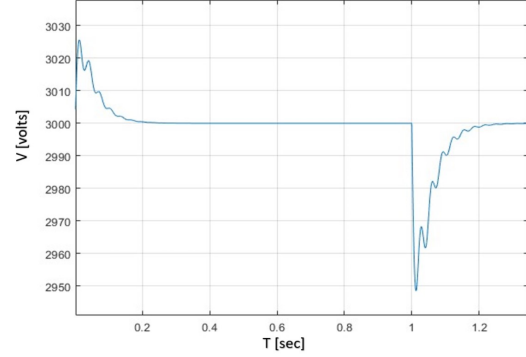


Figure 7 Voltage dynamics on 3 kV bus due to power flow change

As can be seen in the graph, the change in power flow caused a voltage drop on the DC link and the inverter has managed to restore the 3 kV reference on the DC link. It is unexpected for the inverter to lose stability, but the main focus would be on two main points: 1) The over/undershoot value of the voltage, as the overshoot value is critical for the insulation of different equipment such as cables, and undershoot is critical for the stability of converter 2.

B. Converter 2

Converter 2 is a 200 kW interconnection of LV and MV DC grid with a 3 kV input voltage and 1.4 kV output voltage. The main control objective is to maintain a constant voltage on the 1.4 kV (LV DC) side. Since converter 2 is in-house designed, it is possible to optimize its dynamic response through control parameter tuning. For that and for the sake of the stability analysis we consider the converter 2 as an average buck-boost converter with the following equations:

$$V_o = \frac{D}{1-D} \cdot V_{in} \quad (4)$$

$$I_{in} = \frac{D}{1-D} \cdot I_o \quad (5)$$

Where I_{in} and I_o are the input and output currents, I_{in} here represents the input of converter 2 which is the output current of inverter 1. V_{in} and V_o are the input and output voltages where V_{in} is the same as the output voltage of inverter 1. Moreover, D represents the duty cycle. Since the main control objective of the DC-DC converter is to maintain a fixed voltage at the output 1.4 kV DC side, one can say that if inverter 1 provided a stable DC link voltage, where placed physically close to inverter 1 (i.e. low impedance connection line) the duty cycle can be fixed and the output voltage dynamics will follow the dynamics of the DC link between inverter 1 and converter 2. Hence, in this case converter 2 can be represented as a gain. In order to maintain a more stable DC voltage on the 1.4 kV side, we added a PI with a very small K_p value (1×10^{-5}) and $K_i = 0.8$ that can vary the duty cycle based on the variation in the DC link voltage, maintain a more stable voltage around the reference value of 1.4 kV.

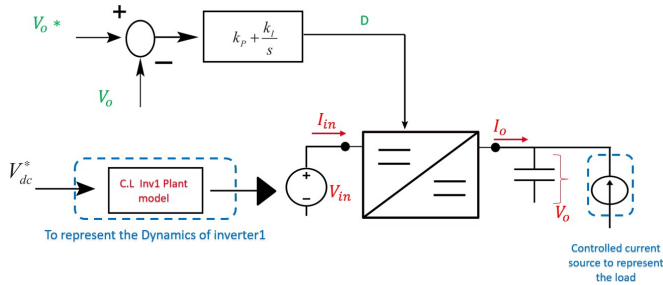


Figure 8 Converter 2 control loop

We then tested a step down of the input voltage (which it the 3 kV DC link controlled by inverter 1 including the dynamics of it, which is done by adding the closed loop equivalent of Figure 5 to observe any dynamical interactions that could lead to instabilities. The results shows that the converter managed to maintain stability with a voltage drop of 3.3% on the input DC-link and. However, due to the dynamics of this change, we see some oscillations on the 1.4 kV, which could cause some problems on the load side based on its nature.

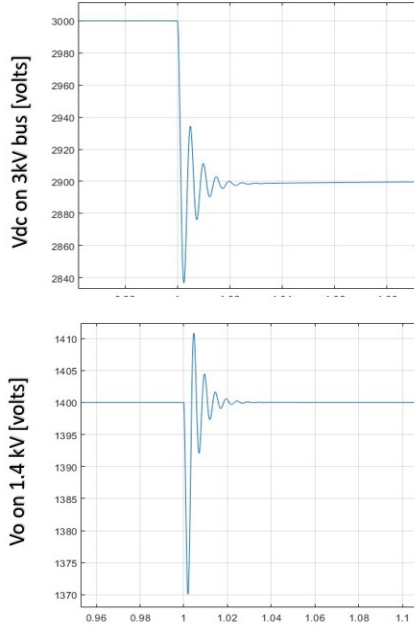


Figure 9 Voltage dynamics on the 1.4 kV bus due to a change on voltage on the 3 kV bus

C. PV and load

The PV solar panels are connected through a DC-DC converter, which uses an MPPT algorithm to inject the maximum available power. This is a commercial product and in this study, we consider the PV as a current source where $I = P_{pv}/V$. V here is considered a constant voltage of 1.4 kV. Load modeled as a dynamic load where we define three main parameters, P_{in} , P_{min} , and V_{min} . P_{actual} is the actual load

consumption that will vary with the following table 2:

Table 2: Model behavior with different values [11]

Applicable range of V values	Applicable range of Pin values	Corresponding Consumed Active Power
$V > V_{min}$	$P_{in} > P_{min}$	$P_{actual} = P_{in}$
	$P_{in} < P_{min}$	$P_{actual} = P_{min}$
$V < V_{min}$	$P_{in} > P_{min}$	$R = V_{min}^2 \frac{P_{actual}}{p_{actual}^2 + Q_{actual}^2}$ $X = V_{min}^2 \frac{Q_{actual}}{p_{actual}^2 + Q_{actual}^2}$ $Z = \sqrt{R^2 + X^2}$
	$P_{in} < P_{min}$	$P_{actual} = P_{min}$

III. STABILITY SIMULATION

Finally, we connect all the elements shown on figure 2 and run a simulation to observe the dynamics of power flow and voltages with two different operational scenarios that can be summarized in the following Table 3: At 0.5 seconds, a load step from 125kW to 100kW and at 1 seconds, a PV production drop from 85kW to 0 kW. Fig. 9-11 show the voltage behaviors in different buses

Table 3: Full model simulation parameters

Variable [initial value]	Event time	New value
P load [125 kW]	T= 0.5 seconds	100 kW
P PV [85e3]	T= 1 seconds	0 kW

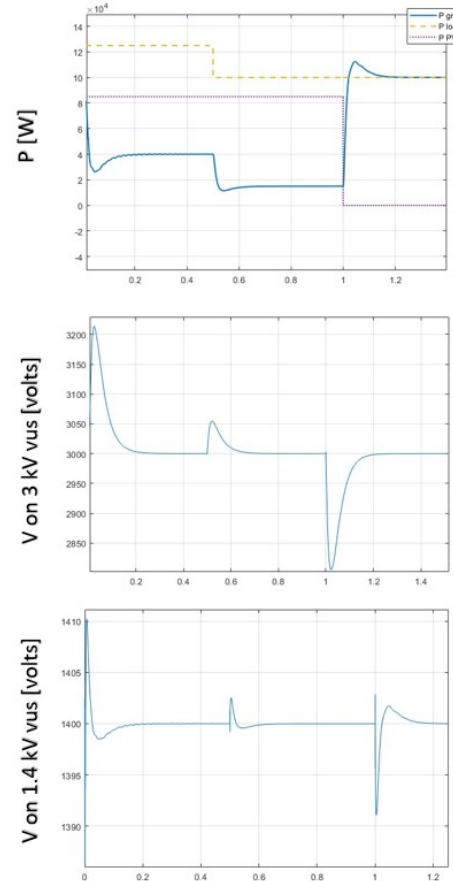


Figure 10 Power and voltage dynamics

As expected, decreasing the load caused an overvoltage on the 1.4 kV bus which was reflected on the 3 kV. Then it was compensated by decreasing the power imported from the grid. The 20% decrease in load caused a 2% voltage overshoot on the 3kV DC link, and a slight overshoot on the 1.4 kV link. An opposite effect is obtained when the system faced a loss of generation (the PV). The system has maintained stability in both tests but special attention should be paid to the values of voltages undershoot or overshoot, especially for expected operational scenarios such as connecting or disconnecting a load. It is worth noting here that in the studied system, converter 2 represents a voltage step-down point, which one can think about it as a buffer or a filter. This means that in some cases by lowering the speed of the outer control loop of converter 2 it can improve the stability of inverter 1 by reducing the overshoot values. One also can think about the size of the DC link capacitor as it also plays a role in this. The main outcome of this stage was to indicate that there were no instabilities due to dynamics interaction in the system and verified that all controllers worked as intended by restoring the referenced set points after disturbances.

IV. DISCUSSION, CONCLUSIONS AND FUTURE WORK

This paper aims to contribute to a DC microgrid demonstration validation through the simulation of its stability analysis. Literature-based models were developed to fulfill the main control objectives of different equipment in the real test case. After that, model verification was made on each piece of equipment using simulation to test the control and to observe the response. Finally, a whole system simulation was done to analyze the system response to two events. Events were chosen to represent a normal operation disturbance and a transient one, which can occur due to a failure in the system. The main purpose of this paper is not to give a definitive answer on the stability of the real test case microgrid; this is due to the lack of full models for different equipment in the network. Rather than that, the main goal is to obtain models, which enable us to indicate critical potential interactions between the two converters' controls. Further simulation will be performed to reinforce the analysis, e.g. sensibility analysis according to the different variables, such as the L1 inductance value in Figure 2 which then makes the inverter's physical locations important at the installation. Scenarios of disturbance events can be also completed, with load step values. A more accurate component model can be developed, once real device experimental characterization can be performed. Finally, due to the simpler control architecture of DC microgrids and the lack of some requirements such as synchronization in comparison with AC microgrids, the stability Analysis of DC microgrids can be simplified. Looking from a system point of view, voltages values on different DC busses can be taken as the main indicator. Due to their relatively smaller sizes (DC microgrids), one must pay attention to the impact of different disturbances on the voltages as a small change can reflect very quickly on the different DC busses which to verify that control response and physical elements such as DC link capacitors are well chosen.

V. REFERENCES

- [1] R. H. Lasseter, 'MicroGrids', in *2002 IEEE Power Engineering Society Winter Meeting. Conference Proceedings (Cat. No.02CH37309)*, New York, NY, USA: IEEE, 2002, pp. 305–308. doi: 10.1109/PESW.2002.985003.
- [2] T. Dragicevic, J. C. Vasquez, J. M. Guerrero, and D. Skrlec, 'Advanced LVDC Electrical Power Architectures and Microgrids: A step toward a new generation of power distribution networks', *IEEE Electrification Mag.*, vol. 2, no. 1, pp. 54–65, Mar. 2014, doi: 10.1109/MELE.2013.2297033.
- [3] B. T. Patterson, 'DC, Come Home: DC Microgrids and the Birth of the "Enernet"', *IEEE Power Energy Mag.*, vol. 10, no. 6, pp. 60–69, Nov. 2012, doi: 10.1109/MPE.2012.2212610.
- [4] L. E. Zubieta, 'Are Microgrids the Future of Energy?: DC Microgrids from Concept to Demonstration to Deployment', *IEEE Electrification Mag.*, vol. 4, no. 2, pp. 37–44, Jun. 2016, doi: 10.1109/MELE.2016.2544238.
- [5] P. Peña-Carro and O. Izquierdo-Monge, 'Hybrid AC/DC architecture in the CE.D.E.R.-CIEMAT microgrid: demonstration of the TIGON project', *Open Res. Eur.*, vol. 2, p. 123, Oct. 2022, doi: 10.12688/openreseurope.15154.1.
- [6] 'TIGON – Demonstrates hybrid AC/DC electricity grid innovations for greener, more resilient and secure power networks'. <https://tigon-project.eu/> (accessed May 22, 2023).
- [7] M. Farrokhhabadi *et al.*, 'Microgrid Stability Definitions, Analysis, and Examples', *IEEE Trans. Power Syst.*, vol. 35, no. 1, pp. 13–29, Jan. 2020, doi: 10.1109/TPWRS.2019.2925703.
- [8] R. Teodorescu, M. Liserre, and P. Rodríguez, *Grid Converters for Photovoltaic and Wind Power Systems*, 1st ed. Wiley, 2011. doi: 10.1002/9780470667057.
- [9] Se-Kyo Chung, 'A phase tracking system for three phase utility interface inverters', *IEEE Trans. Power Electron.*, vol. 15, no. 3, pp. 431–438, May 2000, doi: 10.1109/63.844502.
- [10] J. R. Espinoza, G. Joos, M. Perez, and T. L. A. Moran, 'Stability issues in three-phase PWM current/voltage source rectifiers in the regeneration mode', in *ISIE'2000. Proceedings of the 2000 IEEE International Symposium on Industrial Electronics (Cat. No.00TH8543)*, Cholula, Puebla, Mexico: IEEE, 2000, pp. 453–458. doi: 10.1109/ISIE.2000.930340.
- [11] 'Dynamic load for DC or AC supply - MATLAB - MathWorks France'. <https://fr.mathworks.com/help/sps/ref/dynamicload.html> (accessed May 22, 2023).

VI. ACKNOWLEDGEMENTS

This work has been realized with the participation from members of INES.2S and received funding from the French State under its investment for the future programme with the reference ANR-10-IEED-0014-01 and the support of the Embassy of France in Jordan.